JOURNAL OF THE KOREAN ASTRONOMICAL SOCIETY
39: 151 ~ 155, 2006

FLUX CALIBRATION METHOD OF SLIT SPECTROMETER FOR EXTENDED SOURCES

SUNGHO LEE[1], AND SOOJONG PAK[2]
[1] Korea Astronomy and Space Science Institute, 61-1 Hwaam-dong, Yuseong-gu, Daejeon 305-348, Korea
e-mail: leesh@kasi.re.kr
[2] Department of Astronomy and Space Science, Kyung Hee University, 1 Seocheon-dong, Giheung-gu, Yongin-si, Gyeonggi-do 446-701, Korea
e-mail: soojong@khu.ac.kr
(Received November 12, 2006; Accepted December 20, 2006)

ABSTRACT

Long slit spectrometers are widely used in optical and infrared bands in astronomy. Absolute flux calibration for extended sources, however, is not straightforward, because a portion of the radiation energy from a flux calibration star is blocked by the narrow slit width. Assuming that the point spread function (PSF) of the star is circularly symmetric, we develop a robust method to extrapolate the detected stellar flux to the unobscured flux using the measured PSF along the slit-length direction. We apply this method to our long slit data and prove that the uncertainty of the absolute flux calibration is less than a few percents.

Key words : methods: data analysis — techniques: spectroscopic — infrared: ISM: lines and bands

I. INTRODUCTION

Spectroscopic observation in astronomy is to measure the radiation energy and/or the dynamical parameters of celestial objects. In optical and infrared bands, slit spectrometer is preferable to other spectrometer types, e.g., Fabry-Perot Interferometer and Fourier Transform Spectrometer (Luhman et al. 1994; Pak 2000). Traditionally, astronomical spectroscopy in optical bands has been developed for observing absorption lines from the stellar atmospheres using slit spectrometers. Since the properties of these absorption lines can be characterized by the ratio of the absorbed energy to the continuum energy, i.e., equivalent width, the absolute flux calibration is not required for the most of the stellar spectroscopy.

The grating of the slit spectrometer disperses the radiation perpendicular to the slit length-direction. Since the slit works as a field stop, the slit width controls the amount of throughput energy and the spectral resolution. We need to use the same slit width during observations to keep the same spectral resolution. The full-width at half maximum (FWHM) of the point spread function (PSF), however, depends on the telluric atmospheric seeing condition which is not stable during the observation, and the amount of radiation energy through the slit depends on the PSF. When the observation targets are point sources, e.g, stars and quasars, the absolute flux calibration is just to compare the measured target flux with those of the flux calibration stars (Massey, Valdes, & Barnes 1992). In some special cases when the absolute flux calibration is critical, the targets and the flux calibration stars are measured simultaneously to minimize the effect of the PSF changes (Eigenbrod et al. 2006).

When the targets are extended like galaxies, nebulae, molecular clouds, and planets, the absolute flux calibration becomes troublesome. Astronomers have used two flux calibration methods for extended sources: (1) observing the well-known extended targets, e.g., Orion Nebula, as the flux calibration sources (Hunter & Gallagher 1997) and (2) observing the flux calibration stars with the widest slit which minimizes the masking of the stellar radiation (Pyo 2002). The former method, however, is not reliable because the intensity distribution of a real extended celestial source is not homogeneous and the measured radiation energy depends on the seeing condition. Using the latter method, the spectral resolutions of the target and the calibration star may be different.

In order to calibrate the extended source intensity using the flux calibration star with the same spectral resolution, the measured stellar flux, which is blocked by the slit, needs to be corrected. We develop a robust method to extrapolate the measured stellar flux to the total flux by using the PSF along the slit-length direction. In Section 2, we present the long-slit data which we use for our method. The derived correcting factors are explained in Sections 3 and 4. Finally we discuss the results of our method in Section 5.

II. DATA OF SLIT SPECTROMETER

We used the Cooled Grating Spectrometer 4 (CGS4; Mountain et al. 1990) at the 3.8 m United Kingdom Infrared Telescope (UKIRT) in 2001 and 2003. We configured the CGS4 with a 31 l/mm echelle grating,

Corresponding Author: S. Pak

TABLE 1
STANDARD STARS

Standard star	Observing date (UT)	m_K[a] (mag)	Type[a]	T_{std}[a] (K)	$F_{std}(\lambda_K)$ (W m^{-2} μm^{-1})
HR 6496	2001, 2003/05/23	5.13	F7V	6300	3.67×10^{-12}
BS 6310	2003	4.79[b]	F4V	6600	5.02×10^{-12}

[a] From Eyres et al. 1998.
[b] $m_K = m_H - (H-K)$ where $m_H = 4.83$ (Eyres et al. 1998) and $(H-K) = 0.04$ (Cox 2000).

300 mm focal length camera optics and a two-pixel-wide slit. The pixel scale along the slit was 0.90 arcsec for H_2 1−0 S(1) ($\lambda = 2.1218\mu$m) with the grating angle of 64.°691 and 0.84 arcsec for H_2 2−1 S(1) ($\lambda = 2.2477\mu$m) with 62.°127, respectively; the slit widths on the sky were 0.83 and 0.89 arcsec, respectively, for these two configurations. The slit length is $\sim$ 90 arcsec.

Seeing was less than 1 arcsec throughout the whole observations. The image quality is degraded, however, through the optical system of CGS4 and the final spatial resolution was about 2 arcsec ($\sim$ 0.1 pc at the distance to the Galactic center) according to the FWHM of the flux profile of the standard star along the slit. The instrumental resolutions, measured from Gaussian fits to telluric OH lines in our raw data, were $\sim$ 18 km s^{-1} for H_2 1−0 S(1) and $\sim$ 19 km s^{-1} for H_2 2−1 S(1), respectively.

We observed flux calibration stars, HR 6496 ($\alpha = 17^h27^m2\overset{s}{.}1$, $\delta = -12°30'45''$; J2000) and BS 6310 ($\alpha = 17^h00^m09\overset{s}{.}5$, $\delta = -24°59'21''$; J2000). Table 1 lists the properties of the flux calibration stars. The scientific targets of these observations are the H_2 1−0 S(1) and the H_2 2−1 S(1) emission lines from the central 10 pc of the Galactic center. The near-infrared H_2 emission lines arise from very extended regions where the shocks heat the molecular clouds. The scientific analyses of the data are in the separate papers (Lee et al. 2003; Lee et al. 2006)

III. SLIT OBSCURATION FACTOR

Since only a portion of the flux from the standard star is detected due to the narrow slit (see Figure 1), the measured signal must be corrected for proper flux calibration as

$$F_0 = C_{slit} \cdot F_{obs}. \quad (1)$$

where F_0 is the original unobscured flux of the standard star, F_{obs} is the measured flux, and C_{slit} is the correction factor for the slit obscuration.

Assuming a circularly symmetric PSF for the star, based on the FWHM of the flux profile along the slit length, the intensity distribution is given by

$$I(r) = I_{max} \cdot \exp\left[-\frac{1}{2}\left(\frac{r}{\sigma}\right)^2\right] \quad (2)$$

where I_{max} is the peak intensity and σ = FWHM/2.354. Then the original flux is,

$$\begin{aligned} F_0 &= \int_0^{I_{max}} \pi r^2 \, dI(r) \\ &= 2\pi\sigma^2 I_{max}. \end{aligned} \quad (3)$$

Next we calculate the observed flux after the slit, F_{obs}. When we define x- and y-axis as in Figure 1, since $r^2 = x^2 + y^2$, equation 2 can be written as

$$I(x,y) = I_{max} \cdot \exp\left[-\frac{x^2+y^2}{2\sigma^2}\right]. \quad (4)$$

Given a slit width, $2Y$ (from $-Y$ to Y along the y-axis), the observed flux,

$$\begin{aligned} F_{obs} &= \int_{-Y}^{+Y}\int_{-\infty}^{+\infty} I(x,y)\, dx\, dy \\ &= 2\sqrt{2\pi}\sigma I_{max}\int_0^Y \exp\left[-\frac{y^2}{2\sigma^2}\right] dy. \end{aligned} \quad (5)$$

Noting $u \equiv y/\sqrt{2}\sigma$,

$$F_{obs} = 2\pi\sigma^2 I_{max} \cdot \mathrm{erf}\left(\frac{Y}{\sqrt{2}\sigma}\right), \quad (6)$$

where

$$\mathrm{erf}\left(\frac{Y}{\sqrt{2}\sigma}\right) = \frac{2}{\sqrt{\pi}}\int_0^{\frac{Y}{\sqrt{2}\sigma}} \exp\left[-u^2\right] du. \quad (7)$$

Because error function approaches 1 when Y goes to infinity, one recovers the original flux given in equation 3.

From equations 1, 3, and 6, the slit obscuration factor, C_{slit}, for the missing flux is given by

$$\begin{aligned} C_{slit} &= \frac{F_0}{F_{obs}} \\ &= \mathrm{erf}\left(\frac{Y}{\sqrt{2}\sigma}\right). \end{aligned} \quad (8)$$

This correction factor can be calculated from the slit width ($2Y$) and σ from the seeing size.

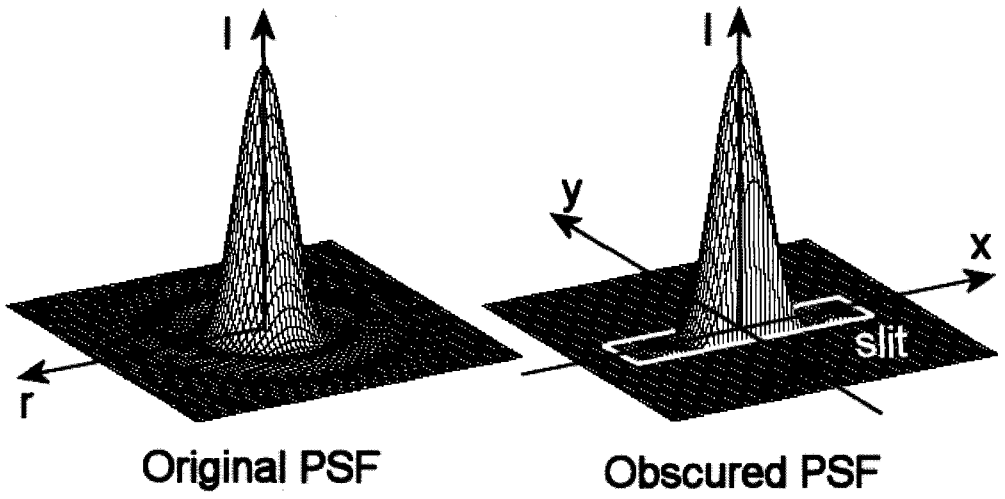

Fig. 1.— Obscuration of a point-spread-function (PSF) by a narrow slit. (left) A circularly symmetric PSF. (right) The PSF obscured by a narrow slit. x-axis is along the slit length and y-axis is along the slit width.

IV. SCALING FACTOR

Flux calibration for extended sources like diffuse H_2 emission from molecular clouds is converting instrumental pixel values in the unit of ADU into specific intensities (I_λ or I_V) in physical units, e.g., W m^{-2} arcsec^{-2} μm^{-1}. Given a pixel value, $S(\lambda)$, the specific intensity, $I(\lambda)$, is calculated by a linear equation,

$$I(\lambda) = C_{flux}(\lambda) \cdot S(\lambda). \quad (9)$$

Here the scaling factor of flux calibration, $C_{flux}(\lambda)$, can be calculated from

$$C_{flux}(\lambda) = \frac{F_{std}(\lambda)}{S_{std}(\lambda)} \cdot \frac{1}{\Omega_{pix}} \cdot \frac{t_{std}}{t_{obj}} \cdot \frac{1}{W_{slit} \cdot C_{slit}} \quad (10)$$

where $F_{std}(\lambda)$ is the flux density of a standard star in W m^{-2} μm^{-1}, $S_{std}(\lambda)$ is the pixel value of the standard star in ADU, Ω_{pix} is the pixel field-of-view (FOV) in arcsec^2, t_{std} and t_{obj} are the exposure times of the standard star and the object, respectively, W_{slit} is the slit width in pixels, and C_{slit} is a correction factor for slit obscuration.

The flux density of a standard star, $F_{std}(\lambda)$, can be calculated if we know its flux density at K-band (2.0–2.4 μm). Since we observe the H_2 lines only in K-band, assuming that the spectral energy distribution of the standard star approximately follows the Planck function in the small range of wavelength, we can use a relation for flux densities like

$$F_{std}(\lambda) = F_{std}(\lambda_K) \cdot \frac{B(\lambda, T_{std})}{B(\lambda_K, T_{std})} \quad (11)$$

where the central wavelength of K-band, $\lambda_K = 2.179$ μm, T_{std} is the effective temperature of the standard star, and the Plank function (Cox 2000) is given by

$$B(\lambda, T_{std}) = \frac{1.1910 \times 10^8 \cdot \lambda_{\mu m}^{-5}}{\exp\left[\frac{14387.7}{\lambda_{\mu m} T_{std}}\right] - 1}. \quad (12)$$

$F_{std}(\lambda_K)$ can be calculated from the K-band flux density of Vega;

$$F_{std}(\lambda_K) = F_{Vega}(\lambda_K) \cdot 10^{-m_K/2.5} \quad (13)$$

where $F_{Vega}(\lambda_K) = 4.14 \times 10^{-10}$ W m^{-2} μm^{-1} (Cox 2000) and m_K is the K-band magnitude of the standard star. We present the information of the standard stars we use in Table 1.

V. RESULTS AND DISCUSSION

For the absolute flux calibration of our CGS4 data we apply the methods described in the previous sections. With the known values of Ω_{pix} ($0\farcs90 \times 0\farcs41 = 0.369$ arcsec^2 for H_2 $1-0$ S(1) and $0\farcs84 \times 0\farcs41 = 0.344$ arcsec^2 for H_2 $2-1$ S(1)), t_{std}/t_{obj} (7/100 for H_2 $1-0$ S(1) and 7/60 for H_2 $2-1$ S(1)), W_{slit} (2 pixels), and C_{slit}, the scaling factors for flux calibration are derived and listed in Table 2.

On the nights of 2001 August 3 and 4, we observed the flux calibration star, HR 6496, before and after each observing night. The measured pixel values, $S_{std}(\lambda)$, changed by $2-7$ % during the same nights because of the seeing changes. Using equation 8, we derive the slit obscuration factors, C_{slit}, based on the PSF profiles along the slit-length direction (see the 6th column in Table 2). Then we calculate the scaling factors, C_{flux}, which directly convert the measured pixel values of the extended targets to the intensity units using

TABLE 2
SLIT OBSCURATION FACTORS AND SCALING FACTORS

Date (UT) (yyyy/mm/dd)	Standard star	$F_{std}(\lambda)$ (W m^{-2} μm^{-1})	$S_{std}(\lambda)$ (ADU)	FWHM (pixel)	C_{slit}	C_{flux} (W m^{-2} arcsec^{-2} μm^{-1} ADU^{-1})
			H_2 1−0 S(1) ($\lambda = 2.1218\mu$m)			
2001/08/03	HR 6496	4.01×10^{-12}	1600	2.13	2.56	9.27×10^{-17}
	HR 6496		1850	1.78	2.20	9.36×10^{-17}
2001/08/04	HR 6496		1480	2.10	2.52	1.02×10^{-16}
	HR 6496		1530	2.00	2.43	1.02×10^{-16}
2003/05/23	HR 6496		2270	2.44	2.94	5.70×10^{-17}
2003/05/28	BS 6310	5.48×10^{-12}	3050	1.80	2.20	7.75×10^{-17}
2003/05/29	BS 6310		2570	2.14	2.59	7.82×10^{-17}
2003/05/30	BS 6310		3480	1.97	2.39	6.24×10^{-17}
2003/05/31	BS 6310		1680	2.19	2.66	1.16×10^{-16}
2003/06/01	BS 6310		3140	1.68	2.06	8.02×10^{-17}
			H_2 2−1 S(1) ($\lambda = 2.2477\mu$m)			
2001/08/04	HR 6496	4.12×10^{-12}	1030	2.02	2.32	1.76×10^{-16}

equation 10. The scaling factors of the same nights agree within $0 - 0.5$ %, which proves that our slit obscuration factors correct the seeing changes almost perfectly.

In equation 10, the ratio of $F_{std}(\lambda)$ to $S_{std}(\lambda)$ includes the detector responsivity which depends on the detector temperature (Rieke 2002) and the atmospheric transmission. Because these parameters change every observing night, the scaling factors in Table 2 are different for different nights. Figure 2 shows two spectral images of the H_2 1−0 S(1) line, which are observed from the same position on the sky but in two different nights; August 3 in 2001 (left) and on May 23 in 2003 (right). After flux calibration using the scaling factors in Table 2, the integrated line intensity of the brightest clump is $\sim 1.8 \times 10^{-17}$ W m^{-2} arcsec^{-2} in the 2001 data and $\sim 1.5 \times 10^{-17}$ W m^{-2} arcsec^{-2} in the 2003 data. The difference of the calibration results is ~ 9 % between the two different seasons over a time gap of about two years. Therefore we conclude that our method is reliable considering that the uncertainty of absolute flux calibration in a near-infrared observation is typically a few tens percent (Pak et al. 2004).

ACKNOWLEDGEMENTS

We thank the referee for many revisions and the insightful interpretation on the formulae. This work was financially supported by grant no. R01-2005-000-10610-0 from the Basic Research Program of the Korea Science and Engineering Foundation.

REFERENCES

Cox A.N., 2000, Allen's astrophysical quantities (4th ed.), AIP press, New York

Eigenbrod, A., Courbin, F., Meylan, G., Vuissoz, C. & Magain, P., 2006, COSMOGRAIL: the COSmological MOnitoring of GRAvItational Lenses. III. Redshift of the lensing galaxy in eight gravitationally lensed quasars, A&A, 451, 759

Eyres S.P.S., Evans A., Geballe T.R., Salama A.,& Smalley B., 1998, Infrared spectroscopy of Sakurai's object, MNRAS, 298, L37

Hunter, D. A., & Gallagher III, J. S., 1997, An Emission-Line Study of Supergiant Ionized Filaments in Irregular Galaxies, ApJ, 475, 65

Lee, S., Pak, S., Davis, C. J., Herrnstein, R. M., Geballe, T. R., Ho, P. T. P., & Wheeler, J. C., 2003, Interaction between the north-eastern boundary of Sgr A East and giant molecular clouds, MNRAS, 341, 509

Lee, S., Pak, S., Choi, M., Davis, C. J., Geballe, T. R., Herrnstein, R. M., Ho, P. T. P., Minh, Y. C., & Lee, S.-G., 2006, Three-dimensional observations of H_2 emission around Sgr A East - I. Structure of the central 10 parsecs, ApJ, submitted

Luhman, M. L., Jaffe, D. T., Keller, L. D., & Pak, S., 1994, H_2 emission as a tracer of molecular hydrogen: Large-scale observations of Orion, ApJ, 436, L185

Massey, P., Valdes, F., & Barnes, J., 1992, A user's guide to reducing slit spectra with IRAF, NOAO

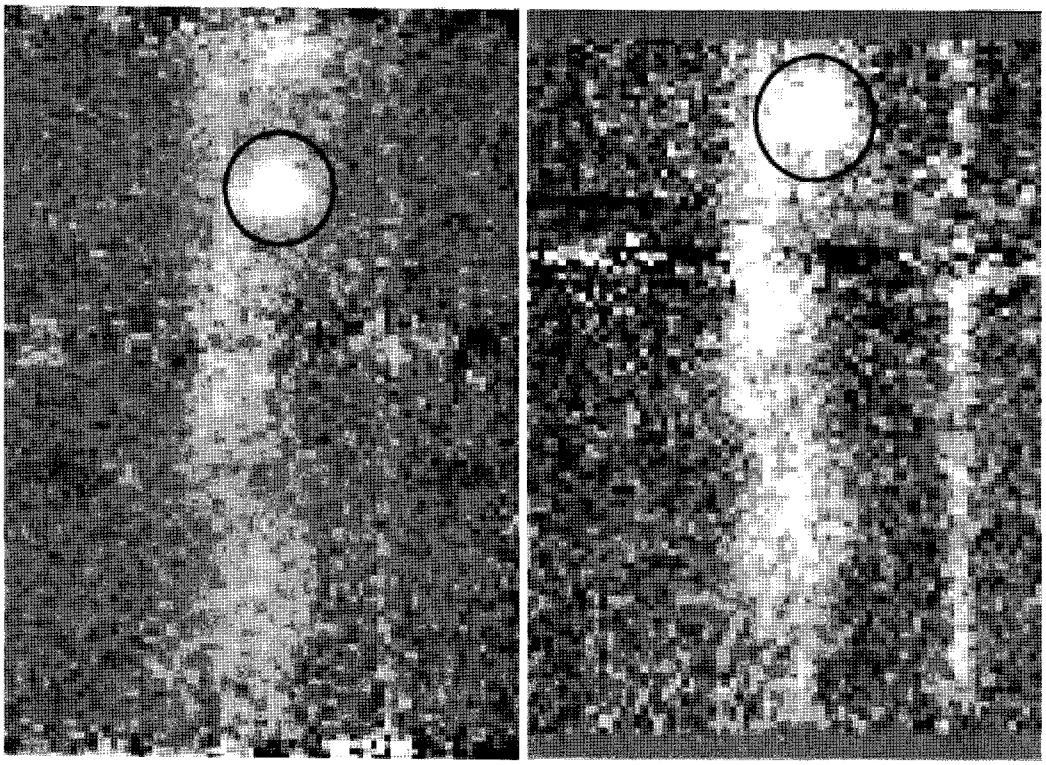

Fig. 2.— Comparison of a common field data in two different nights. Two spectral images of H_2 1−0 S(1) line emission were observed on August 3 in 2001 (left) and on May 23 in 2003 (right), respectively. The vertical direction is along the slit and the direction of spectral dispersion is horizontal. The field position on the sky is $\alpha = 17^h45^m45^s.1$ and $\delta = -28°58'56''$ (J2000), but it was slightly changed along the slit between 2001 and 2003. We compare the integrated intensity of the brightest clump which is marked with a circle in each image (see the text).

Mountain C.M., Robertson D.J., Lee T.J., & Wade R., 1990, An advanced cooled grating spectrometer for UKIRT, in Crawford D.L., ed., Proc. SPIE Vol. 1235, Instrumentation in Astronomy VII. SPIE, Bellingham, p. 25

Pak, S., 2000, Fabry-Perot spectrometer in astronomy, Pub. of the Korean Ast. Soc., 15S, 127

Pak, S., Jaffe, D. T., Stacey, G. J., Bradford, C. M., Klumpe, E. W., & Keller, L. D., 2004, Near-infrared molecular hydrogen emission from the central regions of galaxies: Regulated physical conditions in the Interstellar Medium, ApJ, 609, 692

Pyo, T.-S., 2002, Near infrared [Fe II] spectroscopy of jets and winds emanating from young stellar objects, PhD thesis, University of Tokyo

Rieke, G. H., 2002, Detection of light (2nd ed), Cambridge Univ. Press, Cambridge